

Adaptive curvelet-domain primary-multiple separation

Felix J. Herrmann*, Deli Wang[†] and Dirk J. (Eric) Verschuur[‡]

(January 18, 2008)

Running head: *Curvelet-matched filter*

ABSTRACT

In many exploration areas, successful separation of primaries and multiples greatly determines the quality of seismic imaging. Despite major advances made by Surface-Related Multiple Elimination (SRME), amplitude errors in the predicted multiples remain a problem. When these errors vary for each type of multiple differently (as a function of offset, time and dip), these amplitude errors pose a serious challenge for conventional least-squares matching and for the recently introduced separation by curvelet-domain thresholding. We propose a data-adaptive method that corrects amplitude errors, which vary smoothly as a function of location, scale (frequency band) and angle. In that case, the amplitudes can be corrected by an element-wise curvelet-domain scaling of the predicted multiples. We show that this scaling leads to a successful estimation of the primaries, despite amplitude, sign, timing and phase errors in the predicted multiples. Our results on synthetic and real data show distinct improvements over conventional least-squares matching, in terms of bet-

*Seismic Laboratory for Imaging and Modeling, Department of Earth and Ocean Sciences, University of British Columbia, 6339 Stores Road, Vancouver, V6T 1Z4, BC, Canada

[†]College of Geoexploration Science and Technology, Jilin University, 6 Ximinzhu street, Changchun, 130026, China. Visiting the University of British Columbia.

[‡]Laboratory of Acoustical Imaging and Sound Control, Faculty of Applied Sciences, Delft University of Technology, P.O. Box 5046, 2600 GA, Delft, the Netherlands

ter suppression of multiple energy and high-frequency clutter and better recovery of the estimated primaries.

INTRODUCTION

Surface-Related Multiple Elimination (SRME) (Verschuur et al., 1992; Fokkema and van den Berg, 1993; Berkhout and Verschuur, 1997; Weglein et al., 1997) involves two stages, namely multiple prediction and primary-multiple separation. During the second stage, measures are taken to compensate for imperfections in the multiple predictions. For SRME, predicted multiples often include source signatures and directivity patterns that differ from those present in the data (see e.g. Verschuur et al., 1992; Ikelle et al., 1997). Moreover, 2D SRME produces errors in the predicted multiples due to 3D complexity of the Earth (Dragoet and Jeričević, 1998; Ross et al., 1999; Verschuur, 2006), while recently-developed full 3D-SRME algorithms may suffer from imperfections related to incomplete acquisitions (see e.g. van Borselen et al., 2004; Lin et al., 2004; Moore and Dragoet, 2004; van Dedem and Verschuur, 2005), including erroneous reconstructions of missing near offsets (Dragoet and Jeričević, 1998). For field data, these factors preclude iterative SRME, resulting in amplitude errors that vary for different multiple orders (see e.g. Verschuur and Berkhout, 1997; Pfaffenholz et al., 2002).

In practice, the second separation stage appears particularly challenging since adaptive ℓ_2 -matched-filtering techniques are known to lead to residual multiple energy, high-frequency clutter and deterioration of the primaries (Chen et al., 2004; Abma et al., 2005; Herrmann et al., 2007b). By employing the curvelet transform's ability (Candes et al., 2006; Hennenfent and Herrmann, 2006) to detect wavefronts with conflicting dips (e.g. caustics), Herrmann et al. (2007b,d) were able to derive a non-adaptive (independent of the total data) separation scheme that uses the original data and SRME-predicted multiples as input and produces an estimate for the primaries. This threshold-based method proved robust

with respect to moderate errors (sign, phase and timing) in the predicted multiples, and derived its success from the sparsifying property of curvelets for data with wavefronts. Despite recent advances in thresholding, by a Bayesian formulation (Saab et al., 2007; Wang et al., 2007), and mitigation of the effects of missing data (Herrmann et al., 2007a; Hennent and Herrmann, 2007), curvelet-domain separation deteriorates when the predicted multiples have significant amplitude errors. Thresholding in these cases may give rise to inadvertent removal of primary energy or to remnant multiple energy.

Our contribution: We present a new technique that mitigates the effects of unbalanced amplitudes that vary relatively smoothly along the locations and dips of the predicted multiples. Our approach is complementary to windowed matched-filtering techniques (Verschuur and Berkhout, 1997), which offer limited control over window-to-window variations amongst the estimated matched filters. Our method also avoids relative expensive multiple predictions required by iterative SRME. To offer better control over these variations, errors in the single-window SRME-predicted multiples are modeled by a zero-order pseudo-differential operator, a kind of spatially varying dip filter, which can be well approximated by a diagonal curvelet-domain scaling (Herrmann et al., 2007c). This scaling is estimated from the input data and predicted multiples by a nonlinear optimization procedure, during which smoothness amongst neighboring curvelet coefficients is imposed. This smoothness amongst the curvelet coefficients ensures a scaling that is well-behaved spatially and as a function of the dip. This approach employs the adaptability of curvelets, while the smoothness constraint prevents overfitting of the data, which can lead to a loss of primary energy. Although distinct, our approach is similar to recent work in migration-amplitude recovery, where scaling methods with smoothness constraints have been proposed (Guitton, 2004;

Symes, 2007). This letter builds explicitly on a curvelet-based approach to this problem introduced by Herrmann et al. (2007c).

THEORY

The proposed separation method consists of two stages. During the first adaptive stage, the predicted multiples, $\check{\mathbf{s}}_2$, are fitted through a correction operator to the multiples present in the total data, $\mathbf{p} = \mathbf{s}_1 + \mathbf{s}_2$, which consists of the sum of primaries, \mathbf{s}_1 , and multiples, \mathbf{s}_2 . During the second stage, the primaries and multiples are separated by a thresholding procedure, defined in terms of the scaled magnitudes of the curvelet coefficients of the predicted multiples. Since SRME-predicted multiples are used as input, the wavelet and source directivity will not be properly compensated (Verschuur et al., 1992).

The forward model

Without the wavelet and source directivity, the predicted multiples can be regarded as some scaled (along the time and receiver or offset axes) version of the true multiples. Mathematically, this nonstationary 'scaling' can be represented by a pseudo-differential operator. For our application, this operator acts on shot records or on common-offset panels and applies a location, frequency and dip-dependent zero-phase scaling. By applying a matrix-vector multiplication to the predicted multiples, this operator models the true multiples in the data, i.e.,

$$\mathbf{s}_2 = \mathbf{B}\check{\mathbf{s}}_2, \tag{1}$$

where \mathbf{B} is a full positive-definite matrix, implementing the action of the pseudo-differential operator and $\check{\mathbf{s}}_2$ represents the predicted multiples, calculated with single-windowed con-

volutional matched filtering. Relating the predicted multiples to the true multiples offers flexibility to model amplitude mismatches. Note, however, that this model cannot incorporate kinematic shifts, since pseudo-differential operators are unable to move wavefronts.

By compensating for the source wavelet and directivity, via a conventional local matched-filtering procedure, the pseudo-differential operator becomes zero order and permits a diagonal curvelet-domain decomposition (Herrmann et al., 2007c),

$$\mathbf{s}_2 \approx \mathbf{C}^T \text{diag}\{\mathbf{w}\} \mathbf{C} \check{\mathbf{s}}_2, \quad \{w\}_{\mu \in \mathcal{M}} > 0 \quad (2)$$

with \mathbf{C} the 2D discrete curvelet transform (see e.g. Candes et al., 2006; Hennenfent and Herrmann, 2006) and \mathbf{w} the curvelet-domain scaling vector and \mathcal{M} the index set of curvelet coefficients. Since we are using the curvelet transform based on wrapping, which is a tight frame, we have $\mathbf{C}^T \mathbf{C} = \mathbf{I}$ and the transpose, denoted by the symbol T , equals the pseudo inverse.

In this approximate forward model, for which precise theoretical error estimates exist (Herrmann et al., 2007c), the predicted multiples are linked to the actual multiples by a simple curvelet-domain scaling. This curvelet-domain scaling applies a location, scale and dip dependent amplitude correction. Since the matrix \mathbf{B} is positive-definite, the entries in the scaling vector, \mathbf{w} , are positive. This approximate formulation of the forward model forms the basis for our curvelet-domain matched filter.

Curvelet-domain matched filtering

Equation 2 lends itself to an inversion for the unknown scaling vector. As the true multiples are unknown, our formulation minimizes the least-squares mismatch between the total data and the predicted multiples. The following issues complicate the estimation of the scaling

vector: (i) the undeterminedness of the forward model, due to the redundancy of the curvelet transform, i.e., $\mathbf{C}\mathbf{C}^T$ is rank deficient; (ii) the risk of overfitting the data, which leads to unwanted removal of primary energy, and (iii) the positivity requirement for the scaling vector. To address issues (i-ii), the following augmented system of equations is formed that relates the unknown scaling vector \mathbf{w} to the augmented data vector, \mathbf{d} , i.e.,

$$\begin{bmatrix} \mathbf{p} \\ \mathbf{0} \end{bmatrix} = \begin{bmatrix} \mathbf{C}^T \text{diag}\{\mathbf{C}\check{\mathbf{s}}_2\} \\ \gamma\mathbf{L} \end{bmatrix} \mathbf{w} \quad (3)$$

or $\mathbf{d} = \mathbf{F}_\gamma \mathbf{w}$. The scaling vector is found by minimizing the functional

$$J_\gamma(\mathbf{z}) = \frac{1}{2} \|\mathbf{d} - \mathbf{F}_\gamma e^{\mathbf{z}}\|_2^2, \quad (4)$$

where the substitution of $\mathbf{w} = e^{\mathbf{z}}$ (with the exponentiation taken elementwise) guarantees positivity (issue (iii)) of the solution (Vogel, 2002). This formulation seeks a solution fitting the total data with a smoothness constraint imposed by the sharpening operator \mathbf{L} , which for each scale penalize fluctuations amongst neighboring curvelet coefficients in the space and angle directions (see Herrmann et al., 2007c, for a detailed description). The amount of smoothing is controlled by the parameter γ . For increasing γ , there is more emphasis on smoothness at the expense of overfitting the data (i.e., erroneously fitting the primaries). For a specific γ , the penalty functional in Equation 4 is minimized with respect to the vector \mathbf{z} with the limited-memory BFGS (Nocedal and Wright, 1999) with the gradient

$$\text{grad}J(\mathbf{z}) = \text{diag}\{e^{\mathbf{z}}\} [\mathbf{F}_\gamma^T (\mathbf{F}_\gamma e^{\mathbf{z}} - \mathbf{d})]. \quad (5)$$

Ideally, the solution of the above optimization problem, $\tilde{\mathbf{z}} = \arg \min_{\mathbf{z}} J(\mathbf{z})$, would, after applying the data-dependent scaling, yield the appropriate prediction for the multiples. Unfortunately, other phase and kinematic errors may interfere, rendering a separation based on the residual alone (as in SRME) ineffective, i.e., $\mathbf{p} - \mathbf{C}^T \text{diag}\{\tilde{\mathbf{w}}\} \mathbf{C}\check{\mathbf{s}}_2$ with $\tilde{\mathbf{w}} = e^{\tilde{\mathbf{z}}}$ is

an inaccurate estimate for the primaries. Robustness of threshold-based primary-multiple separation addresses this important issue and forms the second non-adaptive stage of our separation scheme.

Primary-multiple separation by curvelet-domain thresholding

Because of the curvelet’s sparsity and parameterization (by position, scale and dip) primaries and multiples naturally separate in this domain. This property explains the success of threshold-based primary-multiple separation. According to the latest development in threshold-based primary-multiple separation (Saab et al., 2007; Wang et al., 2007), the estimated primaries are given by

$$\tilde{\mathbf{s}}_1 = \text{Bayes}(\mathbf{p}, \mathbf{t}), \quad (6)$$

with the operator $\text{Bayes}(\cdot, \cdot)$ denoting primary estimation by our iterative Bayesian separation scheme (detailed in Saab et al., 2007), which uses the total data and a curvelet-domain threshold vector, \mathbf{t} , as input and which produces the estimated primaries, $\tilde{\mathbf{s}}_1$. This curvelet-domain threshold is given by the absolute values of the (scaled) predicted multiples. Equation 6 is an instance of a non-adaptive curvelet-domain primary-multiple procedure, which as reported in the literature (Herrmann et al., 2007b; Saab et al., 2007; Wang et al., 2007; Herrmann et al., 2007d), has successfully been applied to synthetic- and real-data examples.

APPLICATION

We test the above-described adaptive separation algorithm by examining synthetic and real data. The main purpose of these tests is to study the improvement by curvelet-domain matching compared to optimized results for single-iteration SRME. This case is relevant

for situations where the data quality does not permit iterative SRME or where the cost of multiple iterations of SRME is a concern. In either situation, the predicted multiples will contain amplitude errors, which may give rise to residual multiple energy and dimmed primaries. We show that the proposed scaling by curvelet-domain matched filtering improves the estimation for the primaries as long the curvelet-to-curvelet variations for this scaling are sufficiently controlled by the smoothness constraint. Relaxation of this constraint may lead to overfitting and hence to inadvertent removal of primary energy.

Synthetic-data example

We consider a shot record from a synthetic line, generated by an acoustic finite-difference code for a velocity model that consists of a high-velocity layer, which represents salt, surrounded by sedimentary layers and a water bottom that is not completely flat (see Fig. 11 in Herrmann et al., 2007b). In Figure 1, the results for optimized single-term SRME are compared to curvelet-domain Bayesian separation with and without our amplitude scaling. Figures 1(a)-1(c) include the total input data with multiples, the SRME-predicted multiples and the “multiple-free” data, respectively. The predicted multiples are the result of conventional matching in a single window. The “multiple-free” data were modeled with an absorbing boundary condition, removing the surface-related multiples. Results for the estimated primaries according to optimized single-term SRME with windowed matching, Bayesian separation and scaled-Bayesian separation are included in Figures 1(d)-1(f). Comparison of these results shows a significant improvement for the primaries computed with the curvelet-domain amplitude scaling, calculated by solving Equation 4 for $\gamma = 0.5$. For this choice of γ , the multiples are not over fitted and the amplitude correction leads to a removal of remnant multiple energy, in particular for the events annotated by the arrows.

The value for γ was found experimentally. Finally, notice that the improvement in the estimate for the primaries is due to the combination of curvelet-domain separation and scaling, yielding results that are comparable to the ones expected from multi-term SRME. Even though multi-term SRME, in combination with standard ℓ_2 -subtraction, is known to near perfectly remove surface-related multiples for synthetic data, SRME in practice is often only viable for one iteration because field data sets often do not obey assumptions of the model. Therefore, the single-term SRME result in Figure 1(d) can be considered as state of the art.

Real-data example

Figure 2(a) contains the common-offset section (at offset 200 m) that we selected from a North Sea field dataset. Estimated primaries according to conventional SRME are plotted in Figure 2(b). Results where ℓ_2 -matched filtering in the shot domain (Verschuur and Berkhout, 1997) is replaced by Bayesian thresholding (Saab et al., 2007) in the offset domain, are presented for a single offset in Figure 2(c), without scaling, and in Figure 2(d) with scaling. The scaled result is calculated for $\gamma = 0.3$. Juxtaposing the standard SRME and the curvelet-based results shows a removal of high-frequency clutter, which is in agreement with earlier findings reported in the literature. Moreover, primaries in the deeper part of the section (e.g. near the lower-two arrows in each plot) are much better preserved, compared to the standard-SRME result. Removal of the strong residual multiples in the shallow part, e.g. the first- and second-order water bottom multiples indicated by the arrows around 0.75 and 1.20 s, is particularly exciting. Due to the unbalanced amplitudes of the predicted multiples, both standard SRME and non-adaptive Bayesian thresholding are not able to eliminate these events. Our adaptive method, however, successfully removes these

events by virtue of the curvelet-domain scaling. Compared to non-adaptive thresholding, residual multiples are better suppressed, while our adaptive scheme also leads to at least similar, but often even better, overall continuity and amplitude preservation of the estimated primaries. For example, improvements are visible in the lower-left corner of the sections (between offsets $[0 - 2000]$ m and times $[3.0 - 3.6]$ s), where low-frequency multiple residuals are better suppressed after curvelet-domain matched filtering (cf. Figure 2(c) and 2(d)), without deterioration of the primary energy. Finally, observe the improved recovery of primary energy at the lower arrow in Figure 2(d), compared to the primary in Figure 2(c).

CONCLUSIONS

We presented a method that improves estimates for the primaries for situations where multi-term SRME is unviable. Our alternative augments Bayesian primary-multiple separation with a data-adaptive step, during which the amplitudes of the predicted multiples are matched to the multiples in the data. This match is achieved in the curvelet domain, which allows for a position, scale and dip-dependent amplitude correction through a diagonal scaling of the transform coefficients. Overfitting, i.e., distortion of the primaries, during the matching is avoided by promoting smoothness amongst neighboring coefficients in the scaling vector. Application of our method to synthetic and real-data sets shows a clear improvement in multiple suppression and primary preservation, which can be attributed to the curvelet-domain amplitude correction by scaling. Since our correction is based on a relatively mild smoothness assumption, stating that the amplitude errors can not vary too rapidly as a function of position, scale and angle, we envisage applications in other areas, such as the suppression of internal multiples, where angle-dependent reflection and transmission errors play a role.

ACKNOWLEDGMENTS

The authors would like to thank R. Saab and O. Yilmaz for developing the Bayesian thresholding technique and C.C. Stolk for his implementation of the curvelet-domain smoothness constraint. We also would like to thank the authors of CurveLab (www.curvelet.org). The plots were prepared with Madagascar (rsf.sf.net). The matched-filter method was implemented in scientific python (www.scipy.org) with PyCurveLab (<https://wave.eos.ubc.ca/Software/Licenced/>). Norsk Hydro is thanked for the field dataset. This work was in part financially supported by the NSERC Discovery (22R81254) and CRD Grants DNOISE (334810-05) of F.J.H. and was carried out as part of the SINBAD project with support, secured through ITF, from BG Group, BP, Chevron, ExxonMobil and Shell.

REFERENCES

- Abma, R., N. K. amnd K. H. Matson, S. Michell, S. A. Shaw, and B. McLain, 2005, Comparisons of adaptive subtraction methods for multiple attenuation: The Leading Edge, **24**, 277–280.
- Berkhout, A. J. and D. J. Verschuur, 1997, Estimation of multiple scattering by iterative inversion, part I: theoretical considerations: Geophysics, **62**, 1586–1595.
- Candes, E. J., L. Demanet, D. L. Donoho, and L. Ying, 2006, Fast discrete curvelet transforms: SIAM Multiscale Modeling and Simulation, **5**, 861–899.
- Chen, J., E. Baysal, and O. Yilmaz, 2004, Surface related multiple attenuation on the Sigsbee2B dataset: 74th Ann. Internat. Mtg., SEG, Expanded Abstracts, 1329–1332, Soc. Expl. Geophys., Expanded abstracts.
- Dragoset, W. H. and Z. Jeričević, 1998, Some remarks on multiple attenuation: Geophysics, **63**, 772–789.
- Fokkema, J. T. and P. M. van den Berg, 1993, Seismic applications of acoustic reciprocity: Elsevier.
- Guitton, A., 2004, Amplitude and kinematic corrections of migrated images for nonunitary imaging operators: Geophysics, **69**, 1017–1024.
- Hennenfent, G. and F. J. Herrmann, 2006, Seismic denoising with non-uniformly sampled curvelets: IEEE Computing in Science and Engineering, **8**, 16–25.
- , 2007, Simply denoise: wavefield reconstruction via coarse nonuniform sampling: Geophysics. (Accepted for publication).
- Herrmann, F., D. Wang, and G. Hennenfent, 2007a, Multiple prediction from incomplete data with the focused curvelet transform: SEG International Exposition and 77th Annual Meeting, 2505–2509.

- Herrmann, F. J., U. Boeniger, and D. J. Verschuur, 2007b, Nonlinear primary-multiple separation with directional curvelet frames: *Geophysical Journal International*, **170**, 781–799.
- Herrmann, F. J., P. P. Moghaddam, and C. C. Stolk, 2007c, Sparsity- and continuity-promoting seismic imaging with curvelet frames: *Appl. Comput. Harmon. Anal.* (To appear, doi:10.1016/j.acha.2007.06.007).
- Herrmann, F. J., D. Wang, G. Hennenfent, and P. Moghaddam, 2007d, Curvelet-based seismic data processing: a multiscale and nonlinear approach. (Accepted for publication in *Geophysics*).
- Ikelle, L., G. Roberts, and A. Weglein, 1997, Source signature estimation based on the removal of first-order multiples: *Geophysics*, **62**, 1904–1920.
- Lin, D., J. Young, Y. Huang, and M. Hartmann, 2004, 3-D SRME application in the gulf of mexico: 74th Ann. Internat. Mtg., SEG, Expanded Abstracts, 1257–1260, Soc. Expl. Geophys., Expanded abstracts.
- Moore, I. and W. Dragoset, 2004, 3-D surface-related multiple prediction (SMP): 74th Ann. Internat. Mtg., SEG, Expanded Abstracts, 1249–1252, Soc. Expl. Geophys., Expanded abstracts.
- Nocedal, J. and S. J. Wright, 1999, *Numerical optimization*: Springer.
- Pfaffenholz, J., B. McLain, and P. Keliher, 2002, Subsalt multiple attenuation and imaging: Observations from the Sigsbee2B synthetic dataset: 72th Ann. Internat. Mtg., SEG, Expanded Abstracts, 2122–2125, Soc. Expl. Geophys., Expanded abstracts.
- Ross, W. S., Y. Yu, and F. A. Gasparotto, 1999, Traveltime prediction and suppression of 3-D multiples: *Geophysics*, **64**, 261–277.
- Saab, R., D. Wang, O. Yilmaz, and F. J. Herrmann, 2007, Curvelet-based primary-multiple

- separation from a bayesian perspective: SEG International Exposition and 77th Annual Meeting, 2510–2514.
- Symes, W. W., 2007, Optimal scaling for reverse time migration: Geophysics. (To appear).
- van Borselen, R., R. Schonewille, and R. Hegge, 2004, 3-D srme: Acquisition and processing solutions: 74th Ann. Internat. Mtg., SEG, Expanded Abstracts, 1241–1244, Soc. Expl. Geophys., Expanded abstracts.
- van Dedem, E. J. and D. J. Verschuur, 2005, 3-D surface-related multiple prediction: A sparse inversion approach: Geophysics, **70**, V31–V43.
- Verschuur, D. J., 2006, Seismic multiple removal techniques: past, present and future,; EAGE publications B.V.
- Verschuur, D. J. and A. J. Berkhout, 1997, Estimation of multiple scattering by iterative inversion, part II: practical aspects and examples: Geophysics, **62**, 1596–1611.
- Verschuur, D. J., A. J. Berkhout, and C. P. A. Wapenaar, 1992, Adaptive surface-related multiple elimination: Geophysics, **57**, 1166–1177.
- Vogel, C., 2002, Computational Methods for Inverse Problems: SIAM.
- Wang, D., R. Saab, O. Yilmaz, and F. J. Herrmann, 2007, Recent results in curvelet-based primary-multiple separation: application to real data: SEG International Exposition and 77th Annual Meeting, 2500–2504.
- Weglein, A. B., F. A. Carvalho, and P. M. Stolt, 1997, An inverse scattering series method for attenuating multiples in seismic reflection data: Geophysics, **62**, 1975–1989.

LIST OF FIGURES

1 Primary-multiple separation on a synthetic shot record. **(a)** The total data, \mathbf{p} , including primaries and multiples. **(b)** Single-term SRME-predicted multiples wavelet-matched within a global window ($\check{\mathbf{s}}_2$). **(c)** Reference surface-related multiple-free data modeled with an absorbing boundary condition. **(d)** Estimate for the primaries, yielded by optimized one-term SRME computed with a windowed-matched filter. **(e)** Estimate for the primaries, computed by Bayesian iterative thresholding with a threshold defined by $\mathbf{t} = |\mathbf{C}\check{\mathbf{s}}_2|$. **(f)** The same as **(e)** but now for the scaled threshold, i.e., $\mathbf{t} = |\text{diag}\{\tilde{\mathbf{w}}\}\mathbf{C}\check{\mathbf{s}}_2|$ (with $\gamma = 0.5$). Notice the improvement for the scaled estimate for the primaries, compared to the primaries yielded by SRME in **(d)** and by the Bayesian separation without scaling in **(e)**.

2 Adaptive curvelet-domain primary-multiple separation on real data. **(a)** Near-offset (200 m) section for the total data plotted with automatic-gain control. **(b)** Estimate for the primaries, yielded by optimized one-term SRME computed with a windowed-matched filter. **(c)** Estimate for the primaries, computed by Bayesian iterative thresholding with a threshold defined by $\mathbf{t} = |\mathbf{C}\check{\mathbf{s}}_2|$. **(d)** The same as **(c)** but now for the scaled (for $\gamma = 0.3$) threshold, i.e., $\mathbf{t} = |\text{diag}\{\tilde{\mathbf{w}}\}\mathbf{C}\check{\mathbf{s}}_2|$. Notice the improvement for the scaled estimate for the primaries, compared to the primaries yielded by SRME in **(b)** and by the Bayesian separation without scaling in **(c)**.

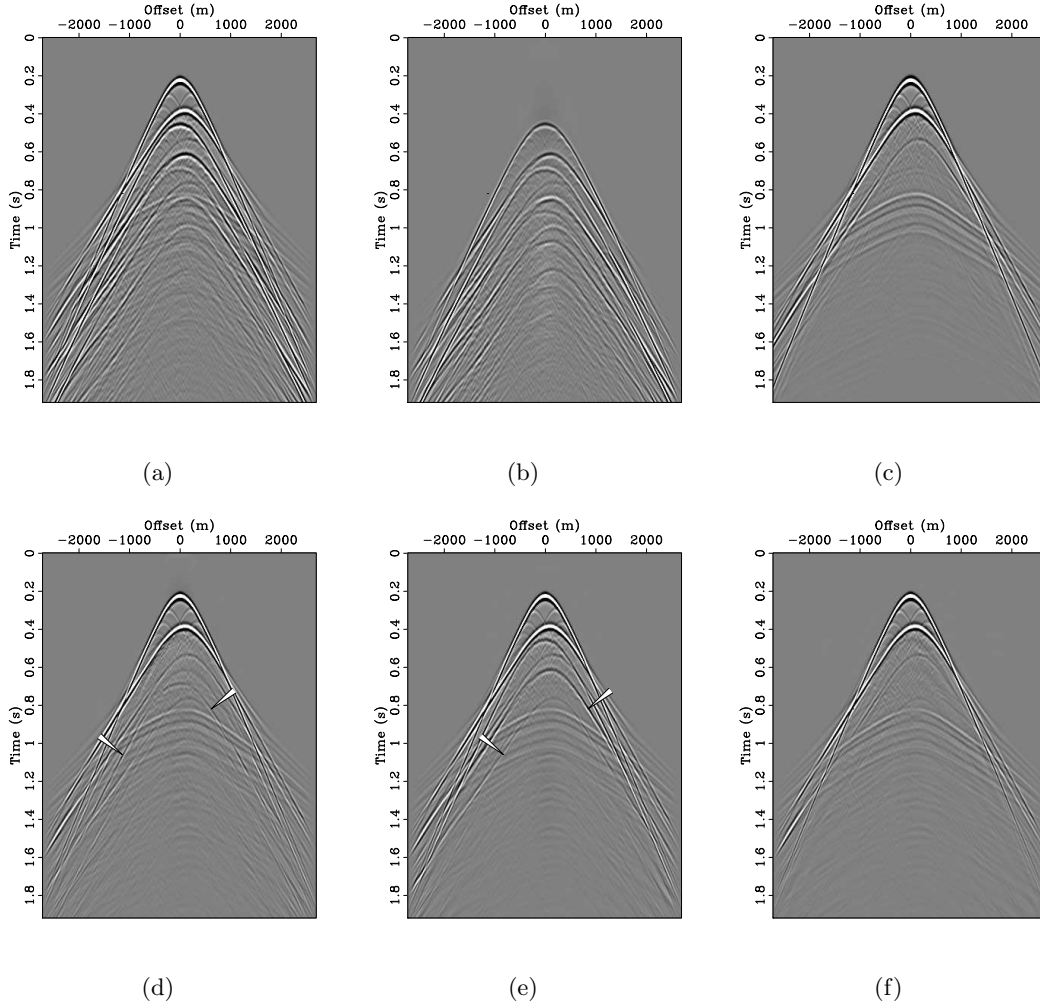


Figure 1: Primary-multiple separation on a synthetic shot record. **(a)** The total data, \mathbf{p} , including primaries and multiples. **(b)** Single-term SRME-predicted multiples wavelet-matched within a global window ($\check{\mathbf{s}}_2$). **(c)** Reference surface-related multiple-free data modeled with an absorbing boundary condition. **(d)** Estimate for the primaries, yielded by optimized one-term SRME computed with a windowed-matched filter. **(e)** Estimate for the primaries, computed by Bayesian iterative thresholding with a threshold defined by $\mathbf{t} = |\mathbf{C}\check{\mathbf{s}}_2|$. **(f)** The same as **(e)** but now for the scaled threshold, i.e., $\mathbf{t} = |\text{diag}\{\tilde{\mathbf{w}}\}\mathbf{C}\check{\mathbf{s}}_2|$ (with $\gamma = 0.5$). Notice the improvement for the scaled estimate for the primaries, compared to the primaries yielded by SRME in **(d)** and by the Bayesian separation without scaling in **(e)**.

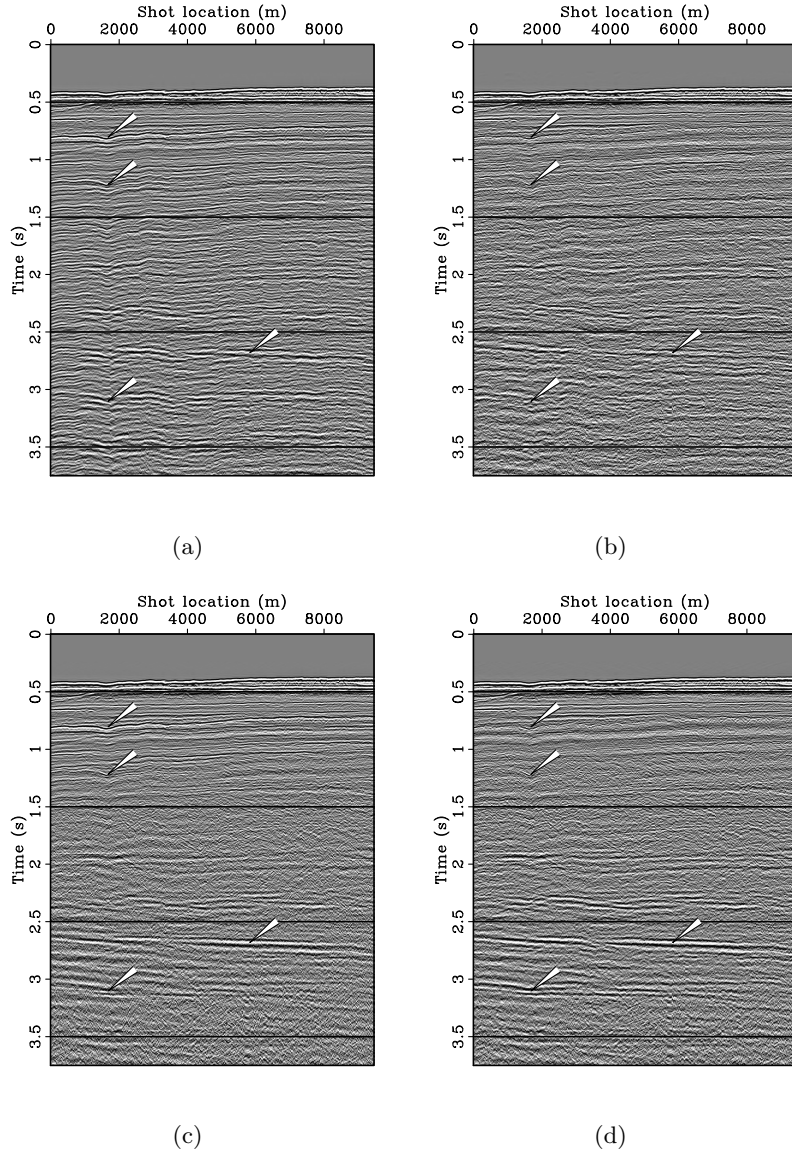


Figure 2: Adaptive curvelet-domain primary-multiple separation on real data. **(a)** Near-offset (200 m) section for the total data plotted with automatic-gain control. **(b)** Estimate for the primaries, yielded by optimized one-term SRME computed with a windowed-matched filter. **(c)** Estimate for the primaries, computed by Bayesian iterative thresholding with a threshold defined by $\mathbf{t} = |\mathbf{C}\check{\mathbf{s}}_2|$. **(d)** The same as **(c)** but now for the scaled (for $\gamma = 0.3$) threshold, i.e., $\mathbf{t} = |\text{diag}\{\tilde{\mathbf{w}}\}\mathbf{C}\check{\mathbf{s}}_2|$. Notice the improvement for the scaled estimate for the primaries, compared to the primaries yielded by SRME in **(b)** and by the Bayesian separation without scaling in **(c)**.